Distribution Agreement

In presenting this thesis as a partial fulfillment of the requirements for a degree from Emory University, I hereby grant to Emory University and its agents the non-exclusive license to archive, make accessible, and display my thesis in whole or in part in all forms of media, now or hereafter now, including display on the World Wide Web. I understand that I may select some access restrictions as part of the online submission of this thesis. I retain all ownership rights to the copyright of the thesis. I also retain the right to use in future works (such as articles or books) all or part of this thesis.

Pulkit Gupta April 1, 2023

Investigation of mitochondrial fusion-mediated T cell expansion and persistence for cancer immunotherapy applications

by

Pulkit Gupta

Mala Shanmugam, PhD

Adviser

Biology

Mala Shanmugam, PhD

Adviser

Roger Deal, PhD

Committee Member

Edmund Waller, MD, PhD

Committee Member

Sumin Kang, PhD

Committee Member

2023

Investigation of mitochondrial fusion-mediated T cell expansion and persistence for cancer immunotherapy applications

By

Pulkit Gupta

Mala Shanmugam, PhD

Adviser

An abstract of

a thesis submitted to the Faculty of Emory College of Arts and Sciences

of Emory University in partial fulfillment

of the requirements of the degree of

Bachelor of Science with Honors

Biology

2023

Abstract

Investigation of mitochondrial fusion-mediated T cell expansion and persistence for cancer immunotherapy applications

By Pulkit Gupta

Chimeric antigen receptor (CAR)-T cell therapy targeting the surface antigen CD19 is an exciting novel therapy for B-chronic lymphocytic leukemia (B-CLL), but CAR-T cell exhaustion remains a challenge for the therapy's efficacy. It is known that mitochondrial biogenesis and metabolism are necessary for robust T cell immune responses and T cell memory and that increased numbers of $CD8^+$ memory T cells are associated with higher responses to CD19 CAR-T therapy. Here, I test the hypothesis that increased mitochondrial fusion improves the survival/expansion of T cells and overcomes T cell exhaustion. In the present study, I utilize a newly-identified mitofusin (MFN) agonist, MASM7, as a tool compound to examine this hypothesis. T cells were isolated from normal donor and B-CLL patient donor peripheral blood mononuclear cells and activated with CD3/CD28 beads. Activated cells were then stimulated with IL-2 treatment and expanded over the course of eight days, with and without MASM7 treatment. Endpoint analysis was performed via fluorochrome-conjugated antibody staining and flow cytometry analysis. Additionally, Seahorse cellular energetics assays, mitochondrial membrane potential staining, and mitochondrial morphology assays were conducted to verify the activity of the drug. Though MASM7 was shown to increase mitochondrial membrane potential and mitochondrial remodeling in multiple different cell types, there were no significant differences in expansion, immune inhibitory checkpoint molecule expression, and activation marker expression between MASM7-treated T cells and vehicle-treated T cells. The current findings suggest that activation of mitochondrial fusion with MASM7 does not improve T cell expansion and persistence. However, further work is required to assess the effects of MASM7 on sustained maintenance of mitochondrial fusion and use of an optimal extrinsic environment for expansion and development.

Investigation of mitochondrial fusion-mediated T cell expansion and persistence for cancer immunotherapy applications

By

Pulkit Gupta

Mala Shanmugam, PhD

Adviser

A thesis submitted to the Faculty of Emory College of Arts and Sciences

of Emory University in partial fulfillment

of the requirements of the degree of

Bachelor of Science with Honors

Biology

2023

Acknowledgements

My biggest thanks goes to Dr. Mala Shanmugam for her continued support and guidance as my advisor through the course of my thesis work. I especially appreciate my committee members Dr. Roger Deal, Dr. Edmund Waller, and Dr. Sumin Kang for their support leading up to my defense. From the Shanmugam group, I want to thank Dr. Remya Nair for her help with the Seahorse metabolic assay and for providing multiple myeloma L363 and KMS18 cells for me to use in the MASM7 activity tests. The rest of Dr. Shanmugam's lab—Dr. Richa Sharma, Dr. Pratik Shriwas, An Vu, Labdhi Mehta, and Shree Allada—have also been instrumental in providing encouragement, asking questions, and contributing feedback for my project. From the Waller group, I want to thank Passang Fnu, Kevin Chen, and Dr. Shuhua Wang for helping me get started with the T cell expansion and flow cytometry analysis protocols and for providing the necessary reagents—B-CLL patient samples, duvelisib, T cell isolation kits, etc.—to carry out those experiments. Lastly, I would like to express gratitude for the help provided by Dr. Evripidis Gavathiotis and Dr. Emmanouil Zacharioudakis from the Department of Biochemistry at Albert Einstein College of Medicine in providing us with the MASM7 drug made in-house and for their assistance with usage of the compound.

Table of Contents

List of Figures

1. Introduction

1.1: B-CLL and CD19 CAR-T therapy

The hematological disease B-chronic lymphocytic leukemia (B-CLL) is a malignancy of B lymphocytes that is the most common adult leukemia in the Western world[1-4]. As a first line therapy, patients with B-CLL are typically administered Bruton's tyrosine kinase inhibitors and/or the anti-apoptotic BCL-2 antagonist venetoclax[5]. Nevertheless, there is still a considerable number of patients who face high-risk disease, drug resistance, and relapse after multiple therapies[6-8]. Chimeric antigen receptor (CAR)-T cell therapy is a relatively new immunotherapeutic strategy in which patient-derived T cells are genetically engineered to express receptors specific for surface proteins expressed on cancer cells[9]. When these CAR-T cells are reintroduced into a patient and activated via binding of the CAR-T cell receptor to the corresponding cancer cell antigen, the CAR-T cells mount a cytotoxic immune response, releasing cytotoxic granules that lead to cancer cell death. CAR-T cell therapy with CARs specific to the B-cell surface protein CD19 has already been FDA-approved as a third-line treatment for diffuse large B-cell lymphoma, B-acute lymphoblastic leukemia, mantle cell lymphoma, and follicular lymphoma[10-13], and BCMA CAR-T cell therapy has been FDA-approved as a fifth-line treatment for multiple myeloma[14]. CD19 CAR-T cell therapy represents an exciting novel therapy for B-CLL[4], but unfortunately, CAR-T cell exhaustion remains a challenge for the therapy's efficacy in B-CLL, leading to cancer cell survival and ineffective treatment[15-20].

Previous work has shown that increased abundance of $CD45RO^{-}$ $CD27^{+}$ $CD8^{+}$ memory T cells in patient peripheral blood is associated with higher complete response to CD19 CAR-T therapy[16]. It is also known that CAR-T exhaustion is associated with changes in T-cell metabolism:

increased T-cell senescence is associated with decreased PPARγ coactivator 1α (PGC1α, the master regulator of mitochondrial biogenesis) expression in activated $CD8^+$ T cells from B-CLL patient donors[17]. Additionally, there is an association of increased mitochondrial number with T-cell fitness[21], and clinically, the mitochondrial mass of infused $CD8^+$ CAR-T cells is linked to more robust B-CLL patient outcomes[17]. Altogether, these studies underscore the importance of metabolism in T cell immune responses and suggest that boosting mitochondrial biogenesis and expanding memory T cell subsets during the manufacture of CAR-T cells is essential for improving B-CLL clinical CD19 CAR-T efficacy.

1.2: PI3K dual-inhibition therapy for T cell persistence

Another class of targeted therapy for B-CLL includes the PI3K-AKT signaling pathway inhibitors idelalisib (PI3Kδ inhibition) and duvelisib (PI3Kδ/γ inhibition), which are both FDA-approved for relapsed/refractory B-CLL[22]. However, it is known that clinical administration of these inhibitors leads to toxicity via T cell-mediated autoimmunity[22-24], likely due to increased T cell expansion and survival with idelalisib as shown in previous ex vivo studies with healthy donor and diffuse large B-cell lymphoma patient-derived T cells[25]. Based on this knowledge, the Edmund Waller group, in collaboration with the Mala Shanmugam group, at Emory University hypothesized that PI3K inhibition can lead to increased persistence in CAR-T cells, and they ultimately showed that dual-inhibition of the PI3K δ and γ isoforms with duvelisib during CAR-T cell manufacturing leads to increased antitumor cytotoxicity[26]. Of importance is the finding that duvelisib-treated T cells exhibit increased memory phenotype, reduced T cell exhaustion, and increased mitochondrial fusion[26].

1.3: Mitochondrial dynamics

Mitochondria are highly dynamic organelles that undergo fission and fusion, allowing for exchange of mitochondrial lipid membranes and proteins for repair of defective mitochondria[27-32]. Additionally, mitochondrial remodeling through fusion and fission is a regulatory mechanism that can help cells adapt to energy demands and extrinsic stress by modulating metabolic activity and programmed cell death[28,33-37]. Mitochondrial fusion generally leads to an increase in mitochondrial membrane potential and oxidative phosphorylation (OXPHOS)[38] through the formation of electron transport chain (ETC) supercomplexes[39], while also limiting the accumulation of damaged mitochondrial DNA[29,40-43]. Fission, on the contrary, leads to fragmented mitochondria and is associated with reduced function, mitophagy, and apoptosis[28,29,32,43-45]. It is known that increased mitochondrial fusion, fatty acid oxidation (FAO), and OXPHOS fuel T cell memory[36,41], and OXPHOS inhibition via complex I-, complex V-, and iron-sulfur cluster-containing protein-inhibition (rotenone, oligomycin, and $CoCl_2$, respectively) has been previously demonstrated to induce T cell exhaustion and reduced proliferation[46]. Furthermore, a metabolic distinguishing feature of terminally exhausted T cells is an increased reliance on aerobic glycolysis[46].

1.4: Mechanisms of mitochondrial fusion and fission

Mitochondrial fusion occurs in a two-step process consisting of outer mitochondrial membrane (OMM) fusion followed by inner mitochondrial membrane (IMM) fusion. OMM fusion is primarily mediated by the mitofusins MFN1 and MFN2, which are localized across the external face of the OMM and are involved in tethering of distinct mitochondria[33,46-50]. Both MFN1 and MFN2 each contain two coiled-coiled heptad repeat (HR) domains (HR1 and HR2) that are involved in regulation of mitofusin activation and mitochondrial tethering[51-54]. The anti-tethering conformation of MFN1/2, characterized by intramolecular HR1-HR2 domain binding, prevents

fusion from occurring. In the pro-tethering conformation of MFN1/2, the HR2 domain is released from the HR1 domain, and fusion is initiated when the free HR2 domain binds to the GTP hydrolase (GTPase) domain of an MFN1/2 molecule on another mitochondrion[53,54]. Fusion initiation also requires either MFN1-MFN2 hetero- or MFN2-MFN2 homo-dimerization across distinct mitochondria[51,53-56]. After OMM fusion, optic atrophy 1 (OPA1), localized in the IMM, mediates IMM fusion and remodels mitochondrial cristae shape, completing the process of fusion[33,39,57,58].

Mitochondrial fission is largely mediated by dynamin-related protein 1 (DRP1), a cytosolic GTPase that is recruited to the OMM when mitochondrial fission is required for cell homeostasis. DRP1 polymerization and accumulation around the mitochondria ultimately lead to recruitment of accessory proteins and eventual compression and splitting of mitochondria[59-61].

1.5: MASM7 is a small-molecule mitochondrial fusion activator

A group at Albert Einstein College of Medicine led by Evripidis Gavathiotis has identified the mitochondrial fusion activator MASM7 via (1) screening of small molecules with an in silico pharmacophore model and (2) experimental validation with mitochondrial length/width as the endpoint[62]. MASM7 mimics HR1 domain residues and exhibits specific binding to the HR2 domain, preventing intramolecular binding of the HR1 and HR2 domains and thus allowing MFN1/2 to remain in the pro-tethering conformation for fusion activation.

A key finding that forms the basis of this study is the Shanmugam and Waller groups demonstrating that administering duvelisib (PI3Kδ/γ inhibition) to CAR-T cells increases mitochondrial content, expands mitochondrial cross-sectional area, raises MFN1 and MFN2

protein levels, and decreases activatory phosphorylation of DRP1[26]. However, they also found no significant differences in the oxygen consumption rates (OCRs, indicative of OXPHOS levels) of duvelisib-treated T cells vs. control T cells, raising the questions of (1) the changes in metabolism that MFN1/2-mediated fusion may be leading to, if not an increase in OXPHOS, and (2) how these metabolic changes confer survival and persistence of the duvelisib-treated T cells. In collaboration with the Waller and Gavathiotis groups, I set out to explore this metabolic basis in the ex vivo expansion of T cells by using MASM7 as a mitochondrial fusion activator to shed light on these research questions.

Work recently completed by Kevin Chen, a Waller/Shanmugam comentee, has shown MASM7 promoting B-CLL patient-derived T cell expansion and mitochondrial fusion[66]. This work serves as a starting point for my hypotheses and experimentation related to the metabolic basis for MASM7-induced expansion.

1.6: MASM7 increases T cell expansion

Peripheral blood mononuclear cells (PBMCs) were isolated from Rai Stage 0-2 B-CLL patients, and T cells were isolated using a human T cell negative isolation kit (as described in Section 2.1). After activation and culturing with DMSO (negative control), MASM7, and duvelisib (positive control) for 48 hours, the T cells were counted. In this preliminary test, treatment with the 5 μM dose of MASM7 was sufficient to induce the expansion of bulk T-cells to levels that were even greater than that of the duvelisib-treated cells (Figure 1).

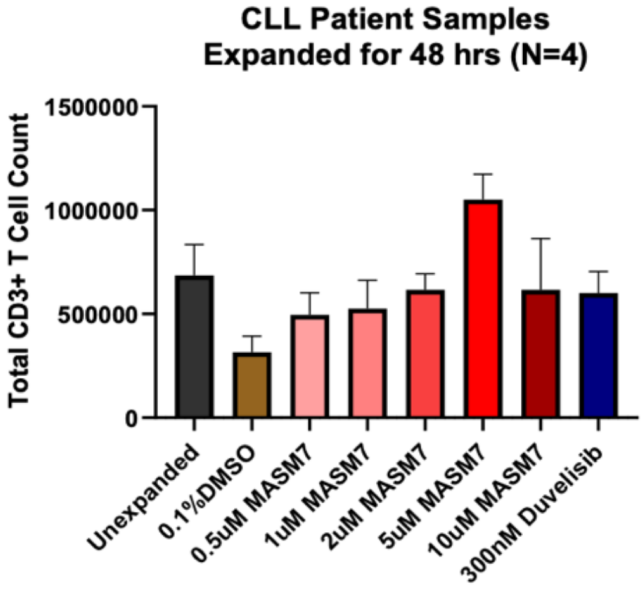

Figure 1: MASM7 expands T cells. CLL patient derived T cells were stimulated on Day 0 with CD3/CD28 beads at a 1:1 cell to bead ratio and expanded in the presence of 300 nM duvelisib or 0.5, 1, 2, 5, or 10 μM MASM7. Following 48 hours of expansion, T cells were counted using Countess® Automated Cell Counter and assayed by flow cytometry. Experiment performed by Kevin Chen[66].

1.7: MASM7 decreases expression of T cell exhaustion markers

To obtain a more clinically relevant time point, further experiments were conducted with endpoints obtained 8 days post-stimulation. Paired comparisons of B-CLL patient derived T cells showed greater expansion with MASM7 treatment as compared to the vehicle control (Figure 2A). The 125 nM MASM7 treatment was sufficient to induce a statistically significant expansion fold difference in the $CD8^+$ subpopulation (Figure 2B) and the $CD8^+$ $CD27^+$ subpopulation (Figure 2C) of T cells. Notably, treatment with MASM7 lowered the frequency of $CD8^+$ T cells co-expressing the TIM3 and LAG3 immune checkpoint molecules, which are also markers of T cell exhaustion[63] (Figure 2D).

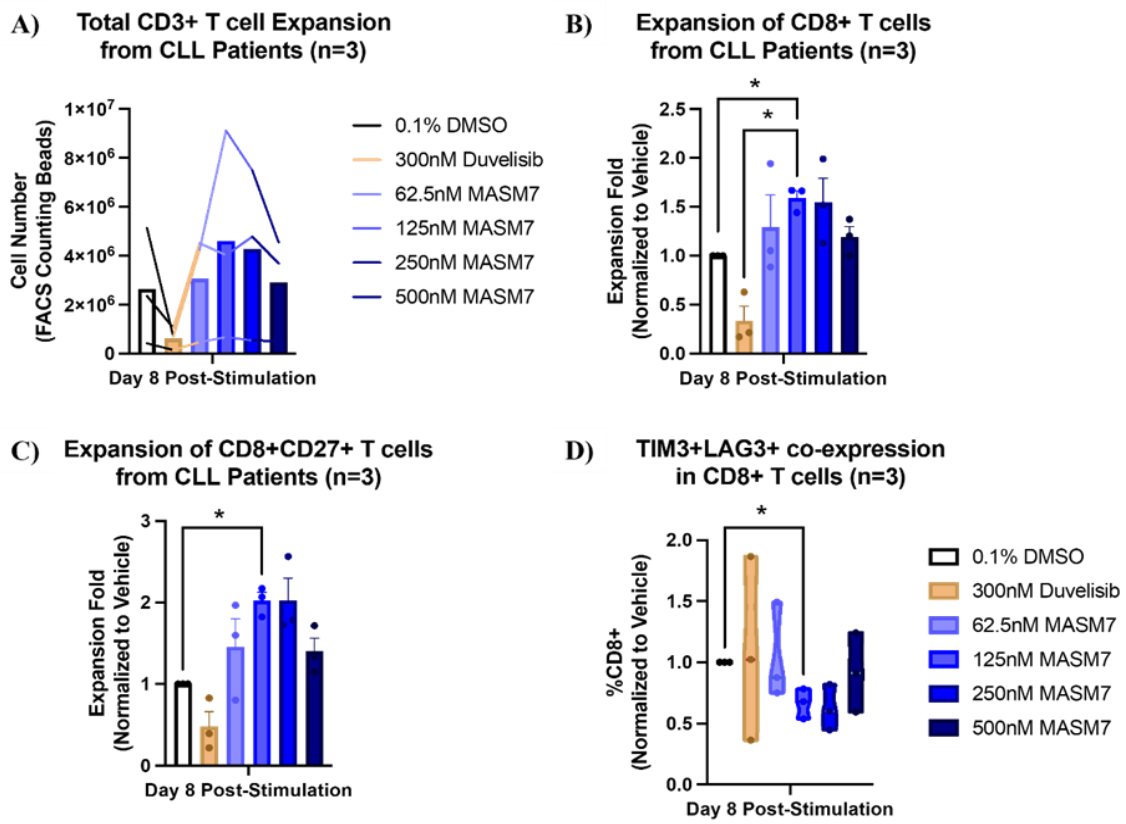

Figure 2: MASM7 augments T cell expansion and decreases exhaustion marker coexpression. T cells from CLL donors were activated with soluble αCD3/CD28 activator, cultured with 0.1% DMSO (vehicle), 300 nM duvelisib, or various doses of MASM7, and immunolabeled for surface marker expression on day 8 of culture. T cell data was acquired on a 4-laser Cytek Aurora spectral cytometer prior to analysis on FlowJo software. Commercial counting beads were used during flow acquisition to calculate cell number. Plots depict **(A)** total number of $CD3^+$ T cells expanded from 200,000 plated cells over the course of 8 days, **(B)** relative expansion of $CD8^+$ T cells, **(C)** relative expansion of $CD8^+$ $CD27^+$ T cells, and **(D)** relative frequency of $TIM3^+$ $LAG3^+$ co-expressing cells within the $CD8^+$ compartment. Relative expansion fold and frequency denote normalization to the vehicle. *$p < 0.05$. Experiment performed by Kevin Chen[66].

1.8: MASM7 increases mitochondrial volume in patient-derived B-CLL T cells

To determine the activity of MASM7 in generating the T cell expansion phenotype, structured illumination microscopy was performed and mitochondrial morphology was assessed (Figure 3A) after eight days of expansion, with the mitochondrial import receptor subunit TOM20 stained as a marker for mitochondria. Mitochondrial volume per mitochondrion was quantified (Figure 3B), and it was found that patient-derived B-CLL T cells treated with 250 nM MASM7 had increased fusion, compared to the vehicle control and duvelisib. Additionally, evaluation of the mitochondrial membrane potential (ψ_m) to mitochondrial mass ratio—indicative of the presence of more functional mitochondria relative to the total amount of mitochondria in each cell—by flow cytometry revealed significant increases with the 125 nM dose of MASM7.

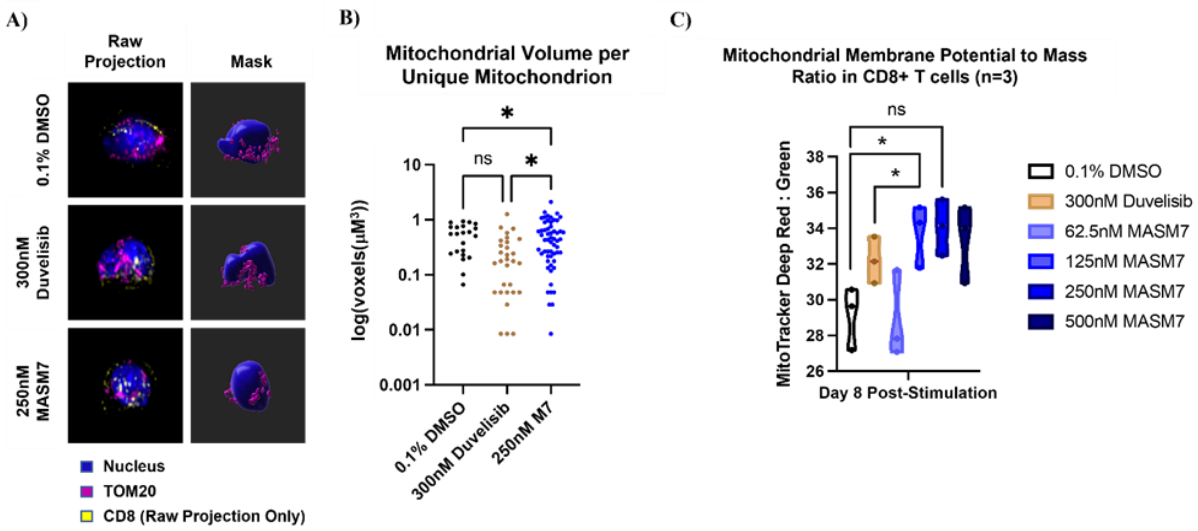

Figure 3: MASM7 augments T cell mitochondrial fusion. T cells from CLL donors were activated with soluble αCD3/CD28 activator, cultured with 0.1% DMSO (vehicle), 300 nM duvelisib, or various doses of MASM7. On day 8 of culture, T cells were harvested, fixed in 4% paraformaldehyde, and stained for surface CD4 (not shown) CD8 (yellow), mitochondrial TOM20 (violet), and nuclear DNA (blue). **(A)** Z-stacks of single-cell, widefield images acquired on a DeltaVision OMX SIM microscope were reconstructed as 3D projections on the left, and nuclei and mitochondria fluorescent signals, but not CD8, were masked to mark distinct organelle borders on the right. **(B)** Mitochondrial volume per

individual/networked mitochondria was quantified using Imaris software and graphed in GraphPad Prism. **(C)** Mitochondrial membrane potential (ψ_m) to mass ratio was evaluated by flow cytometry staining of MitoTracker Deep Red (marker for active mitochondria) and MitoTracker Green (marker for mitochondria, regardless of ψ_m) and plotted in GraphPad Prism. *p < 0.05; ns = not significant. Experiment performed by Kevin Chen[66].

1.9: Research objectives and hypotheses

Altogether, the preliminary data provide evidence for MASM7's specific effects of increasing mitochondrial fusion and total expansion in B-CLL patient derived T cells *ex vivo*. Based on these results, my goal was to optimize the MASM7 expansion protocol for B-CLL T cells and then perform a metabolic assay on the MASM7-treated cells to elucidate the basis for increased T cell expansion. Generally, based on previous studies[36,64,65], I had expected to observe increased OXPHOS and FAO with a decrease in apoptotic pathway activity. I was also aware that sorting of bulk T cells into $CD4^+$ and $CD8^+$ T cells for all experimentation would be crucial for identifying particular subpopulations that are more significantly affected by MASM7 activity.

Thus, the overarching objective of this thesis project is to obtain a preliminary mechanistic understanding of how mitochondrial dynamics modulates T cell expansion.

2. Methods

2.1: T cell isolation and expansion

The workflow diagrammed in Figure 4 was followed for T cell isolation and expansion, with the starting point being frozen PBMCs.

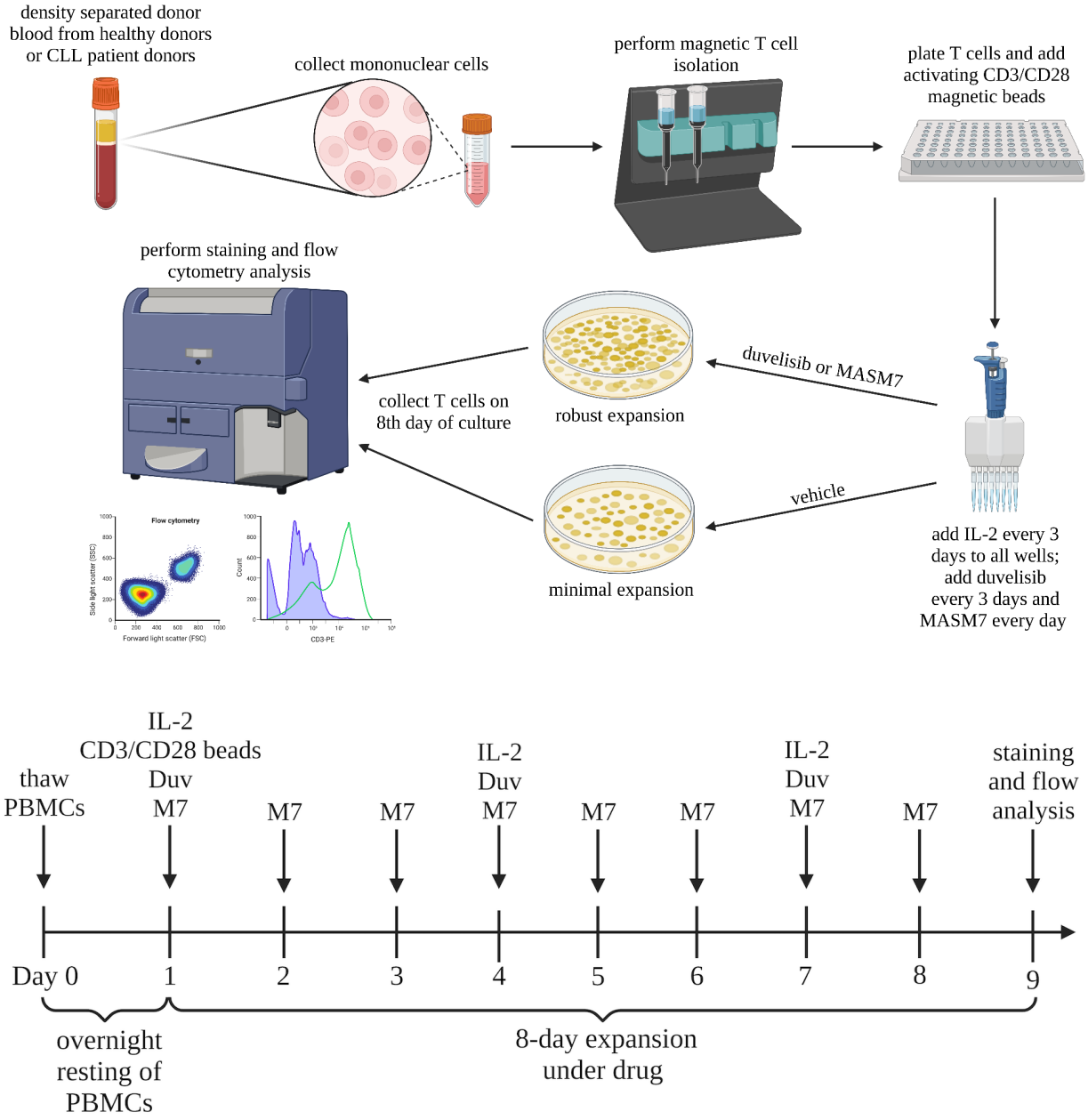

Figure 4: Experimental workflow and timeline for *ex vivo* expansion studies. Frozen PBMCs originating from density-separated donor blood (from 4-5 different patient samples serving as biological

replicates) are thawed and rested overnight in preparation for T cell isolation. The following day, T cells are isolated from the PBMCs with a human T cell negative isolation kit, and they are activated with CD3/CD28 magnetic Dynabeads in a 1:1 bead:cell ratio. IL-2, duvelisib, and MASM7 are added on the first day, with dimethyl sulfoxide (DMSO) acting as the vehicle control. IL-2 and duvelisib are added every 3 days, and MASM7 is added every day. I expected robust expansion to occur with the positive control (duvelisib) and the experimental treatment (MASM7) but not with the negative control (vehicle). After 8 days of culture, the cells were harvested for analysis. *Figure created with BioRender.com.*

2.2: T cell marker staining and flow cytometry analysis

CD3/CD28 magnetic beads were removed from T cells with a separation magnet, and immunostaining was performed with by incubating cells at 4℃ for 30 min with the following fluorochrome-conjugated antibodies: LIVE/DEAD aqua, CD3 PE-CF594, CD4 APC-Cy7, CD8 AF700, PD-1 PE-Cy7, LAG3 PE, TIM3 BV421, CD27 BV650, and CD28 APC.

Flow cytometry was performed on a four-laser Cytek Aurora instrument with at least 10,000 lymphocyte, non-doublet events collected per sample, and cell counts (to assess expansion) were obtained via volumetric counting with a low flow rate. Gating and expression analysis was done on the FCS Express V4 software, and flow-minus-one controls were used to assist with gating. All expression analysis was done with appropriate gating for live cells only. Lastly, statistical analysis was done in GraphPad Prism using two-way ANOVA.

2.3: Cellular energetics assays

Cellular energetics assays were conducted to test the activity of MASM7, and L363 multiple myeloma cells were used instead of T cells. Using a Seahorse XFe24 Metabolic Flux Analyzer with 300,000 cells plated per well, I evaluated OCR and spare respiratory capacity (SRC) after 12 hours of treatment.

2.4: Mitochondrial membrane potential and mitochondrial visualization assays

To assess MASM7 activity, mitochondrial membrane potential was assessed using tetramethylrhodamine, methyl ester (TMRE) dye staining and flow cytometry analysis with KMS18 multiple myeloma cells.

Mitochondrial visualization was achieved with Mitotracker green using SK-MEL-30 melanoma cells and confocal microscopy.

3. Results and Analysis

3.1: MASM7 does not induce expansion of healthy donor-derived T cells

Healthy donor cells—as opposed to B-CLL patient derived cells—were selected as a starting point for ease of access and availability. Frozen PBMCs from healthy donors (n = 5) were thawed and rested overnight, and T cells were isolated the next day. T cells were plated in 96-well round bottom plates with CD3/CD28 activating magnetic beads and were cultured for 7 days, with MASM7 added every day and duvelisib and IL-2 added every 3 days. On the eighth day, T cells were harvested, isolated from magnetic beads, stained with fluorochrome-conjugated antibodies, and analyzed with flow cytometry. Data were analyzed with appropriate gating for live T cells.

$CD8^+$ cytotoxic T cell subsets exhibited no significant increase in expansion with MASM7 at any dose (Figure 5A), and coexpression of the T cell exhaustion markers PD1 and LAG3 (Figure 5B) or PD1 and TIM3 (Figure 5C) were not significantly reduced with MASM7 treatment, though there was a reduction in coexpression with duvelisib. The transcription factor TCF1 is associated with $CD8^+$ effector function, and its expression increases with duvelisib treatment but not with MASM7 (Figure 1D). From these results, I hypothesized that MASM7 did not have any effect on healthy donor cells and proceeded to investigate MASM7's effect on B-CLL patient-derived T cells.

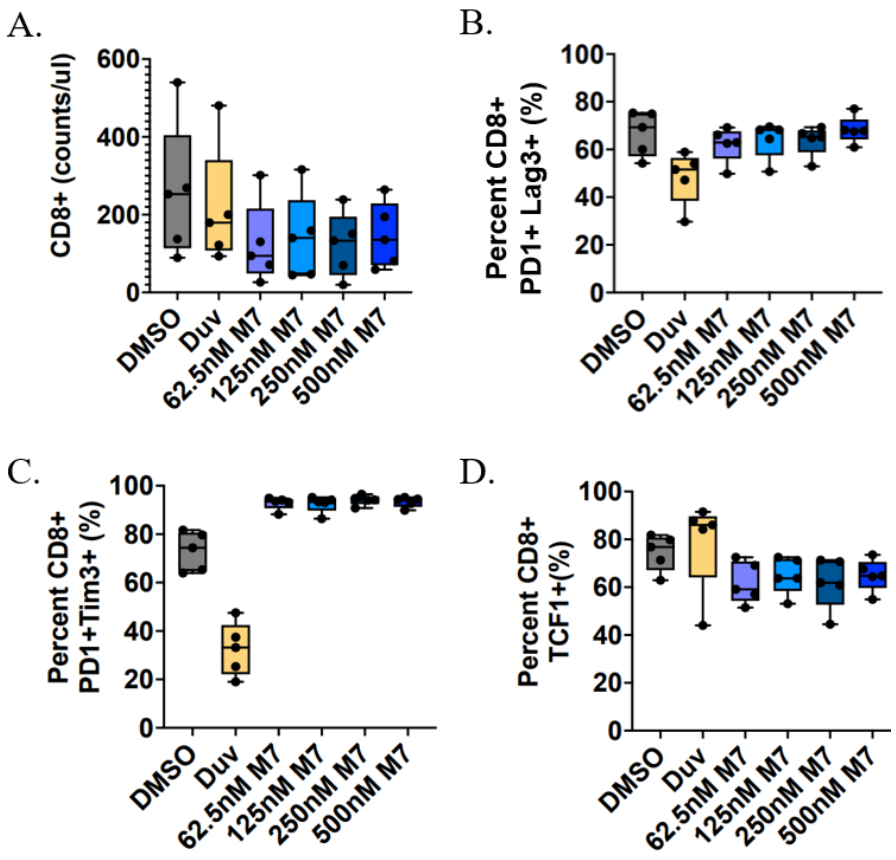

Figure 5: Healthy donor T cells are not able to replicate the MASM7 expansion phenotype. Fluorochrome-antibody staining and flow cytometry analysis after 7 days of T cell culture with 0.1% DMSO, 300 nM duvelisib (duv), or a range of MASM7 (M7) doses is shown. T cells from five healthy donors were used for this experiment. The analysis included **(A)** raw live $CD8^+$ T cell counts, **(B)** co-expression of PD1 and LAG3 as a percentage of total CD8s, **(C)** co-expression of PD1 and TIM3 as a percentage of total CD8s, and **(D)** TCF1 expression in the CD8 population. Experiment performed by Passang Fnu.

3.2: B-CLL patient-derived T cells are not able to replicate the MASM7 expansion phenotype

The same experiment as above was repeated with B-CLL patient-derived frozen PBMCs as a starting point.

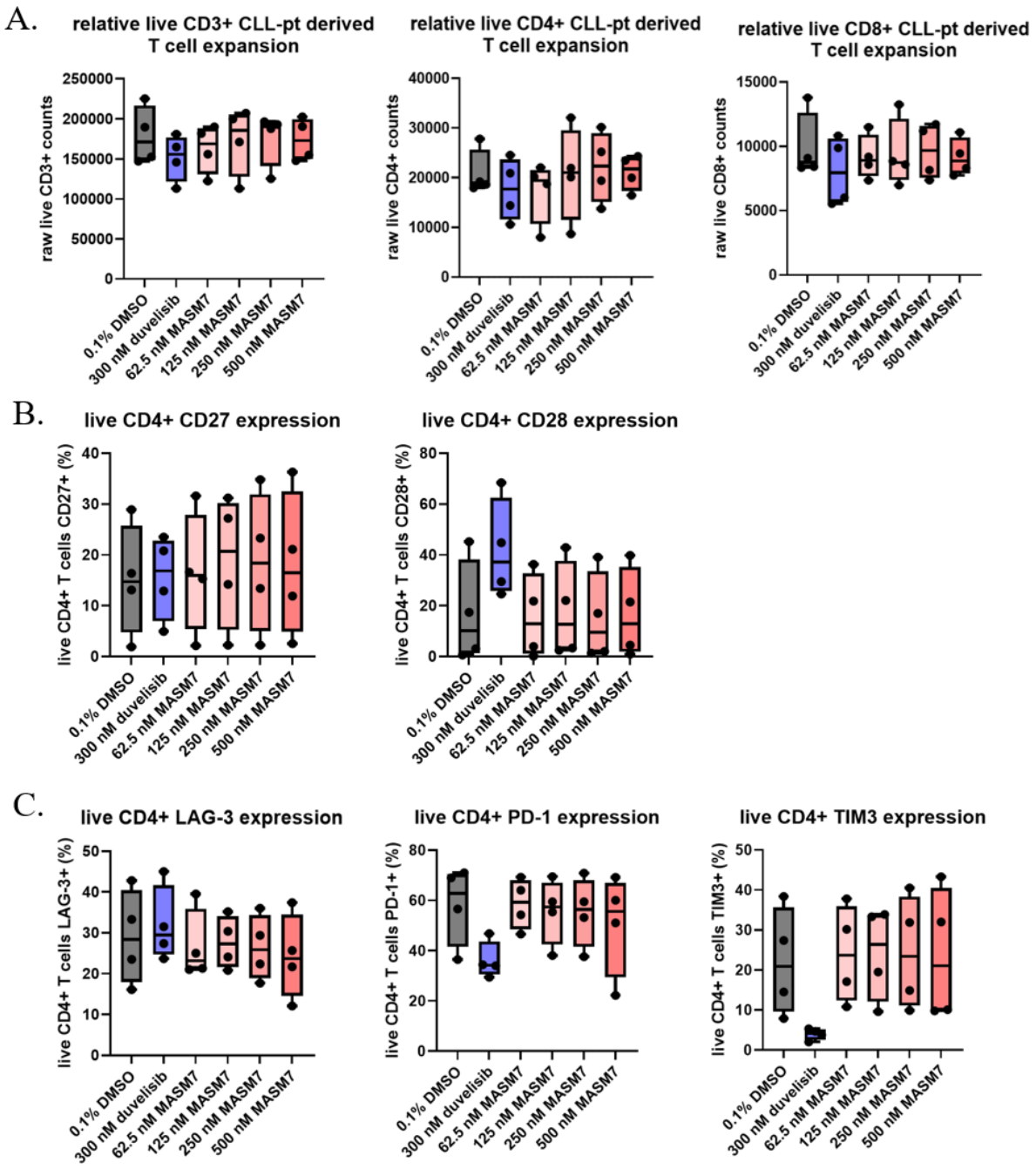

Figure 6: B-CLL patient-derived T cells are not able to replicate the MASM7 expansion phenotype. Fluorochrome-antibody staining and flow cytometry analysis after 8 days of T cell culture with 0.1% DMSO, 300 nM duvelisib, or a range of MASM7 doses. T cells from four B-CLL patient donors were used for this experiment. The analysis included **(A)** expansion across $CD3^+$, $CD4^+$, and $CD8^+$

T cell subsets, **(B)** expression of a panel of activation markers in $CD4^+$ cells, and **(C)** expression of a panel of exhaustion markers in $CD4^+$ cells.

There was no significant expansion in the bulk T cells ($CD3^+$) and in the $CD4^+$ helper T cell/$CD8^+$ cytotoxic T cell subsets (Figure 6A). Additionally, while duvelisib increased CD28 expression in the CD4 subset, none of the MASM7 doses were able to replicate this phenotype (Figure 6B). Lastly, none of the MASM7 doses were able to reduce any of the exhaustion markers, though the PD1 and TIM3 exhaustion markers were reduced with duvelisib treatment (Figure 6C). Analysis of representative plots for TIM3 (Figure 7) reveal very minimal changes with the MASM7 doses compared to the control, as well as a lack of a dose-dependent response to MASM7.

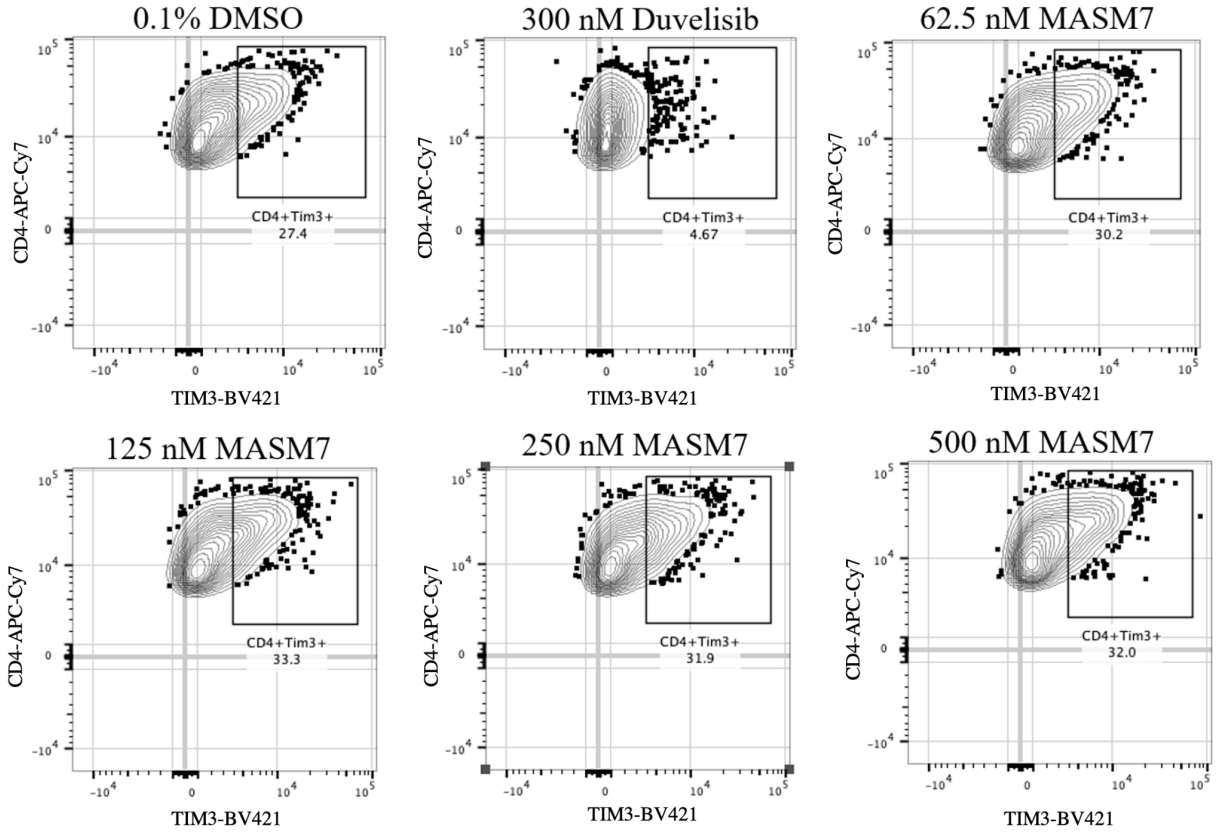

Figure 7: TIM-3 representative flow cytometry expansion plots. APC-Cy7 is the fluorochrome conjugated to the CD4 antibody, and BV421 is the fluorochrome conjugated to the TIM3 antibody.

Given that all of the MASM7 treatments looked similar to the control and that there is an absence of a dose-dependent response for MASM7, I believed that the MASM7 compound may not have been stable, so I reconstituted new MASM7 powder obtained from the Gavathiotis lab in DMSO and tried the experiment again.

3.3: Time course data reveals no significant differences with MASM7 treatment

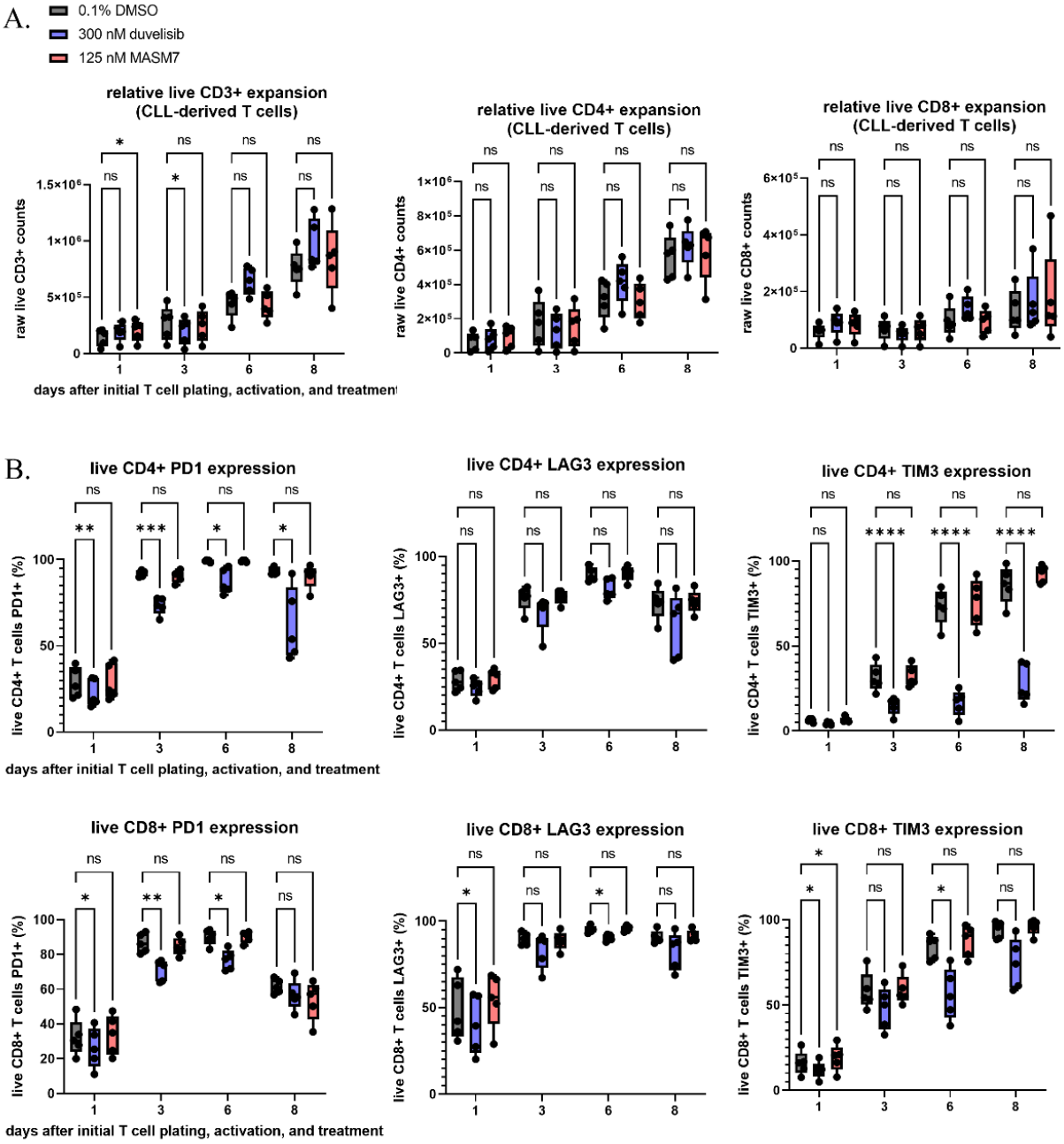

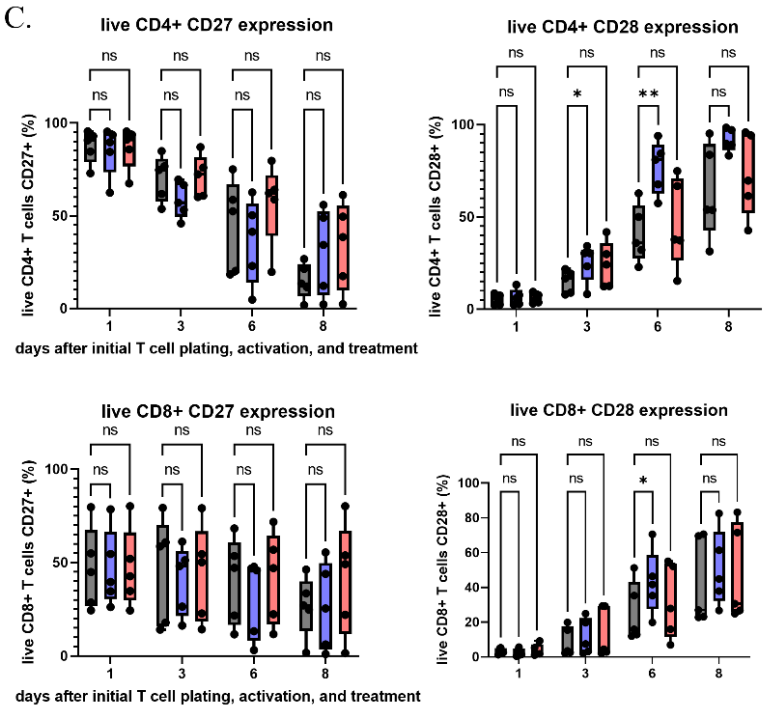

Figure 8: Eight-day time course expansion with MASM7. Fluorochrome-antibody staining and flow cytometry analysis after 1, 3, 6, and 8 days of T cell culture with 0.1% DMSO, 300 nM duvelisib, or 125 nM MASM7 are shown. T cells from five B-CLL patient donors were used for this experiment. The analysis included **(A)** expansion across $CD3^+$, $CD4^+$, and $CD8^+$ T cell subsets, **(B)** activation marker expression in $CD4^+$ and $CD8^+$ cells, and **(C)** exhaustion marker expression in $CD4^+$ and $CD8^+$ cells. *$p \leq 0.05$, **$p \leq 0.01$, ***$p \leq 0.001$, ****$p \leq 0.0001$, ns = not significant.

A time course experiment with 125 nM MASM7 was conducted in which cells were taken out after 1, 3, 6, and 8 days for analysis to determine if MASM7 efficacy is specific to a certain time point. This dose was chosen based on previous data (Figure 1) that suggested that 125 nM is the most efficacious MASM7 dose. Across all time points, there was no meaningful increase in $CD3^+$, $CD4^+$, and $CD8^+$ bulk expansion with MASM7 (Figure 8A), and while duvelisib-treated cells displayed decreased expression of exhaustion markers PD-1, LAG3, and TIM3 for both $CD4^+$ and $CD8^+$ subsets, MASM7 showed no effect on exhaustion marker expression compared

to the control (Figure 8B). Furthermore, both $CD4^+$ and $CD8^+$ populations showed a significant increase in CD28 activation marker expression at the 6-day time point, but MASM7 showed no difference in expression compared to the control (Figure 8C).

Based on these data, I hypothesized that the MASM7 compound used in my experiments was inactive, and I performed a series of experiments to test its efficacy.

3.4: Seahorse experiment provides evidence for inactive MASM7 drug

MASM7 has been previously shown to increase OCR and SRC in mouse embryonic fibroblasts (MEFs) with only 6 hours of treatment in a Seahorse metabolic assay[62]. Based on this data, I endeavored to test the activity of MASM7 with a similar experiment using easily accessible myeloma cells.

Treatment with MASM7 doses ranging from 0.1 μM to 10 μM did not lead to a significant increase in basal oxygen consumption (Figure 9), suggesting that the compound was inactive. This result can be invalidated by MASM7's transient mechanism of action—by replacing the treatment media with Seahorse XF assay media, the effects of MASM7 could have been lost by the time that analysis with the Seahorse machine was conducted. Nevertheless, I obtained more MASM7 drug in another batch that was created in-house from the Gavathiotis group and proceeded to test its activity before trying another T cell expansion with it.

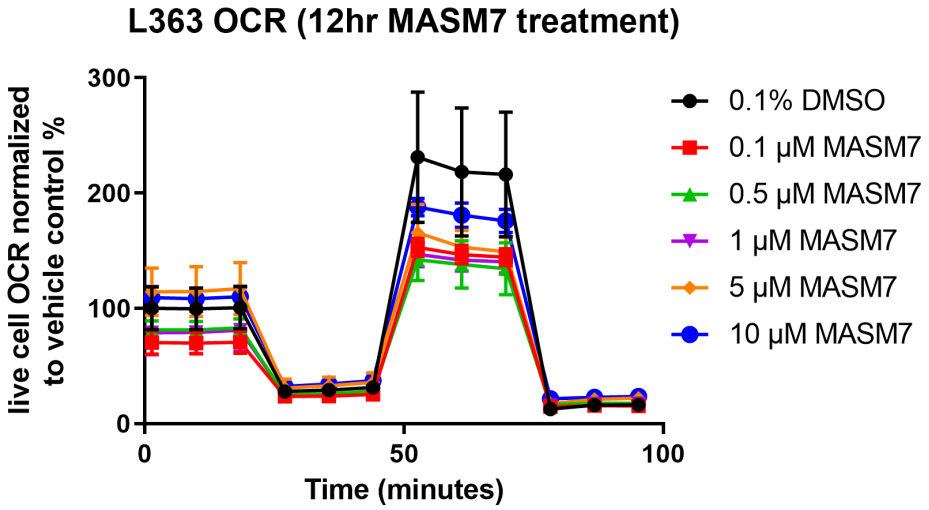

Figure 9: MASM7 compound did not lead to increased OCR or SRC in myeloma cells. L363 myeloma cells were plated with either 0.1% DMSO or a range of MASM7 doses from 0.1 μM-10 μM for 12 hours. Cells were resuspended in Seahorse XF assay media and analyzed with a Seahorse XFe24 Metabolic Flux Analyzer with 300,000 cells plated per well. To measure mitochondrial respiration parameters (basal OCR, SRC, etc.), 1 μM oligomycin, 2 μM carbonyl cyanide-4-(trifluoromethoxy) phenylhydrazone (FCCP), and 1 μM rotenone + 1 μM antimycin were added sequentially at the 20 min, 50 min, and 80 min time points, respectively.

3.5: New MASM7 stock is effective at increasing fusion and ψ_m

Before sending the new batch of MASM7 to me, the Gavathiotis group performed confocal microscopy and Mitotracker Green staining (which stains for mitochondria regardless of mitochondrial membrane potential, ψ_m) on melanoma cells with their new MASM7 batch, showing that the treated cells have increased mitochondrial networks as compared to a vehicle control (Figure 10). MASM7 has already been shown to increase mitochondrial networking with the same assay in MEFs[62], so this served as a positive test for the drug's activity.

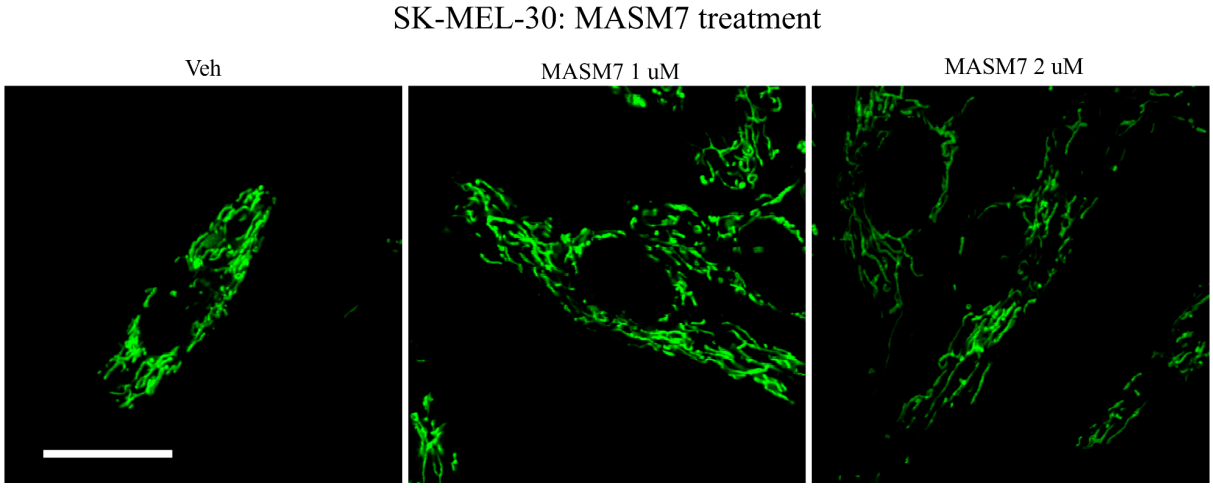

Figure 10: MASM7 increases mitochondrial network formation in melanoma cells. SK-MEL-30 melanoma cells were treated with either 1 µM MASM7, 2 µM MASM7, or a vehicle control, stained with Mitotracker Green, and visualized with confocal microscopy. Scale bar = 20 µm. Experiment performed by Emmanouil Zacharioudakis.

Once I received the drug, I tested its activity with TMRE staining (used to assess ψ_m) and flow cytometry in easily accessible KMS18 multiple myeloma cells. TMRE fluorescence has also been shown to increase with MASM7 treatment after 6 hours in MEFs[62], so I expected an increase in TMRE to be indicative of an active compound. The mitochondrial uncoupler FCCP was used as a control for the experiment. Treatment with the MASM7 compound (January 2023 batch) for 6 hours resulted in increased TMRE for a range of doses (Figure 11).

Given that the drug activity of the new batch of MASM7 was validated with two different techniques (mitochondrial networking visualization and TMRE mitochondrial potential staining) in two different cell types (SK-MEL-30 melanoma and KMS18 multiple myeloma cells), I proceeded to test the compound's efficacy in expanding T cells.

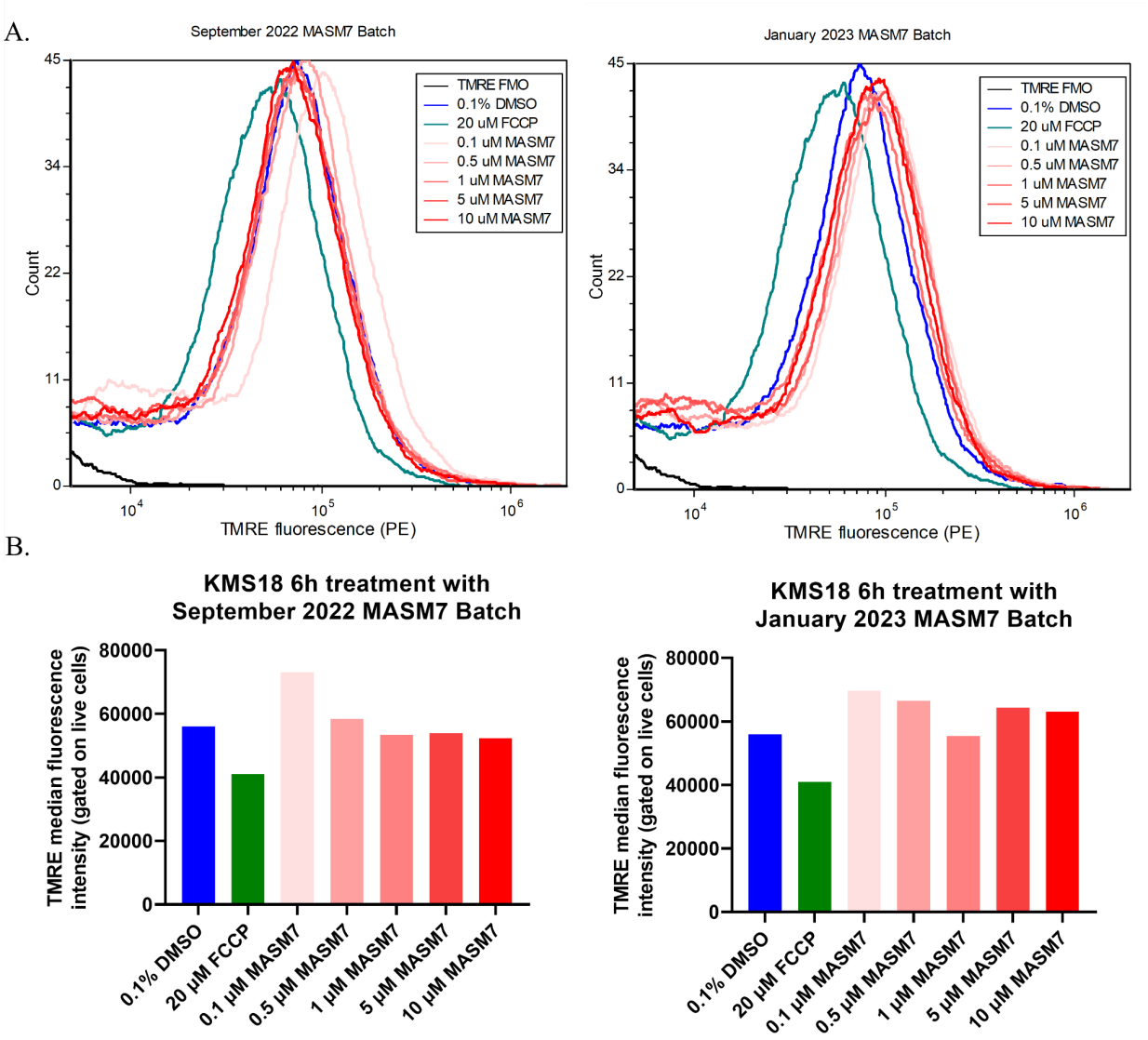

Figure 11: MASM7 increases TMRE staining in myeloma cells. KMS18 cells were treated for 6 hours with either 0.1% DMSO, 20 µM FCCP, or a range of MASM7 doses and then subject to TMRE dye staining and flow cytometry. Two batches of MASM7 were used: one batch produced and received in September 2022 and one batch produced and received in January 2023. All TMRE analysis was gated on live cells. **(A)** TMRE fluorescence histograms and **(B)** quantification of median fluorescence intensity are shown.

3.6: Final MASM7 T cell experiment yields no appreciable differences in expansion

An 8-day T cell expansion experiment was conducted with the new batch of MASM7 drug and the same protocol and MASM7 dose concentrations as used previously.

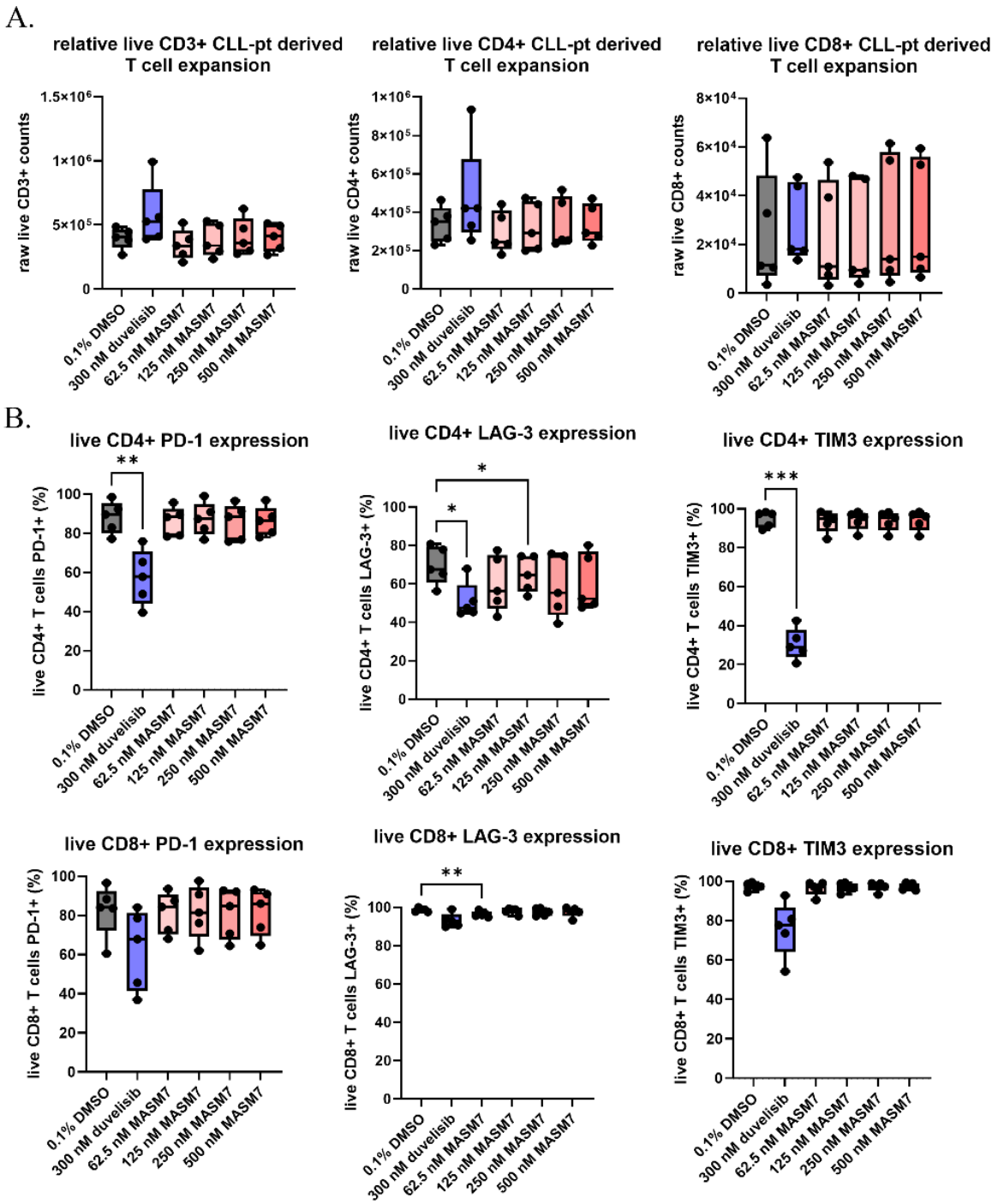

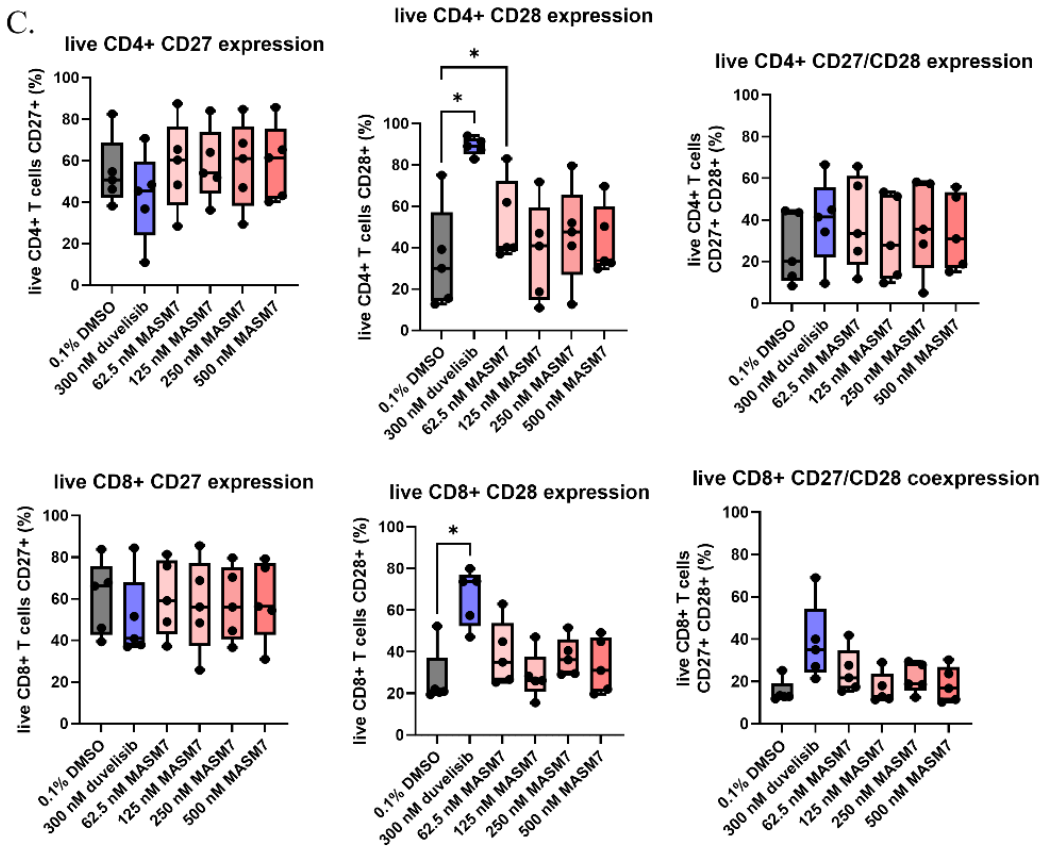

Figure 12: Treatment with new MASM7 compound is not able to replicate the expansion phenotype. Fluorochrome-antibody staining and flow cytometry analysis after 8 days of T cell culture with 0.1% DMSO, 300 nM duvelisib, or a range of MASM7 doses is shown. T cells from five B-CLL patient donors were used for this experiment. The analysis included **(A)** expansion across $CD3^+$, $CD4^+$, and $CD8^+$ T cell subsets, **(B)** activation marker expression in $CD4^+$ and $CD8^+$ cells, and **(C)** exhaustion marker expression in $CD4^+$ and $CD8^+$ cells. *$p \leq 0.05$, **$p \leq 0.01$, ***$p \leq 0.001$, ****$p \leq 0.0001$, ns = not significant.

While the duvelisib-treated cells showed a positive response, there were no appreciable differences in $CD3^+/CD4^+/CD8^+$ T cell expansion (Figure 12A), exhaustion marker expression (Figure 12B), and activation marker expression (Figure 12C) in the MASM7-treated cells in any of the doses tested.

4. Discussion and Conclusions

4.1: Treatment with MASM7 is not sufficient to induce MFN-mediated T cell expansion

Given the emerging importance of CAR-T cell therapy and its utility in providing a personalized, lasting approach to cancer therapy, it is important to investigate the metabolic and signaling pathways that enable T cell function and memory. Though the fusion protein OPA1 has been previously shown to be necessary for T cell memory[36], it is still unclear whether direct modulation of mitochondrial fusion with small molecule agonists has an effect on T cell expansion and memory development and whether these effects can bolster CAR-T therapy responses.

While previous laboratory data has shown a strong effect of MASM7 on B-CLL patient-derived T cell expansion (Figure 1), exhaustion marker reduction (Figure 2), and mitochondrial fusion (Figure 3), I was not able to replicate this effect, even through the use of three separate batches of MASM7 combined with verification that the last batch was active in multiple cell types. Furthermore, the use of duvelisib as a working positive control in the T cell expansion experiments provides additional evidence to suggest a lack of an effect from MASM7. One possible confounding factor that could have accounted for variability and lack of response to MASM7 is that the CLL patient samples used are variable and imatinib resistant, which could have altered their T cell biology.

4.2: Future experimentation

Further studies beyond the scope of this project would examine the utility of MASM7 in boosting the efficacy and persistence of B-CLL patient derived T cells and CAR-T therapy and would examine more specific T cell subpopulations, including the naïve (T_n), stem cell memory

(T_{scm}), central memory (T_{cm}), effector memory (T_{em}), and terminally differentiated effector memory re-expressing CD45RA (T_{emra}) T cell populations. It may be the case that one or more of these populations is affected by MASM7 treatment but has exhaustion/proliferation marker expression that is covered up by noise from other populations in the bulk CD3/CD4/CD8 analysis. Additionally, to better understand the mechanism of fusion-mediated expansion, treatment of cells with low glucose culture, galactose culture, or 2DG (hexokinase inhibitor) could shed more light on the role of OXPHOS in expansion and/or differentiation state reprogramming of these subpopulations since it is known that mitochondrial fusion increases OXPHOS.

To determine the necessity of fusion in expanding memory T cell populations, genetic silencing of the fusion mediators DRP1/MFN1/MFN2 would be used. It is already known that loss of MFN2, but not DRP1 or MFN1, leads to decreased proliferation in the helper-T (T_H) subpopulations T_H1, T_H2, and T_H17 and in the regulatory T cell (T_{reg}) subpopulation and that silencing of MFN2 but not DRP1 or MFN1 leads to decreased OCR in T_H17s[64]. Additionally, culture of T_H17s in conditions conducive to OXPHOS has been shown to result in increased antiapoptotic BCL-xL expression and decreased apoptotic BIM expression, leading to increased persistence[65]. For this reason, it would be useful to probe protein expression levels of a panel of apoptotic proteins to determine whether MASM7-mediated fusion can make cells more resistant to apoptosis, independent of altering exhaustion/activation marker expression.

Lastly, combinations of MASM7 and duvelisib would be explored in the future to determine possible drug synergy in boosting T cell expansion, since it is known that duvelisib increases MFN1/2 expression and promotes epigenetic rewiring that leads to increased T cell stemness and persistence[26].

5. References

1. Bosch F, Dalla-Favera R. Chronic lymphocytic leukaemia: from genetics to treatment. *Nature Reviews Clinical Oncology*. 2019;16(11):684-701. doi:10.1038/s41571-019-0239-8

2. Wierda WG, Brown J, Abramson JS, et al. NCCN Guidelines® Insights: Chronic Lymphocytic Leukemia/Small Lymphocytic Lymphoma, Version 3.2022: Featured Updates to the NCCN Guidelines. *Journal of the National Comprehensive Cancer Network*. 1AD;20(6):622-634. doi:10.6004/jnccn.2022.0031

3. Hallek M. Chronic lymphocytic leukemia: 2020 update on diagnosis, risk stratification and treatment. *American Journal of Hematology*. 2019;94(11):1266-1287. doi:https://doi.org/10.1002/ajh.25595

4. Gribben JG. How and when I do allogeneic transplant in CLL. *Blood*. 2018;132(1):31-39. doi:10.1182/blood-2018-01-785998

5. Woyach JA. Management of relapsed/refractory Chronic Lymphocytic Leukemia. *American Journal of Hematology*. 2022;97(S2):S11-S18. doi:https://doi.org/10.1002/ajh.26683

6. Anderson MA, Tam C, Lew TE, et al. Clinicopathological features and outcomes of progression of CLL on the BCL2 inhibitor venetoclax. *Blood*. 2017;129(25):3362-3370. doi:10.1182/blood-2017-01-763003

7. O'Brien S, Furman RR, Coutre S, et al. Single-agent ibrutinib in treatment-naïve and relapsed/refractory chronic lymphocytic leukemia: a 5-year experience. *Blood*. 2018;131(17):1910-1919. doi:10.1182/blood-2017-10-810044

8. Mato AR, Thompson MC, Nabhan C, Svoboda J, Schuster SJ. Chimeric Antigen Receptor T-Cell Therapy for Chronic Lymphocytic Leukemia: A Narrative Review. *Clinical Lymphoma Myeloma and Leukemia*. 2017;17(12):852-856. doi:10.1016/j.clml.2017.07.007

9. Chavez JC, Bachmeier C, Kharfan-Dabaja MA. CAR T-cell therapy for B-cell lymphomas: clinical trial results of available products. *Therapeutic Advances in Hematology*. 2019;10:2040620719841581. doi:10.1177/2040620719841581

10. S Abramson J, M Lia Palomba, I Gordon L, et al. Lisocabtagene maraleucel for patients with relapsed or refractory large B-cell lymphomas (TRANSCEND NHL 001): a multicentre seamless design study. *The Lancet*. 2020;396(10254):839-852. doi:10.1016/S0140-6736(20)31366-0

11. Neelapu SS, Locke FL, Bartlett NL, et al. Axicabtagene Ciloleucel CAR T-Cell Therapy in Refractory Large B-Cell Lymphoma. *N Engl J Med*. 2017;377(26):2531-2544. doi:10.1056/NEJMoa1707447

12. Schuster SJ, Bishop MR, Tam CS, et al. Tisagenlecleucel in Adult Relapsed or Refractory Diffuse Large B-Cell Lymphoma. *N Engl J Med*. 2019;380(1):45-56. doi:10.1056/NEJMoa1804980

13. Mian A, T. Hill B. Brexucabtagene autoleucel for the treatment of relapsed/refractory mantle cell lymphoma. *Expert Opinion on Biological Therapy*. 2021;21(4):435-441. doi:10.1080/14712598.2021.1889510

14. Raje N, Berdeja J, Lin Y, et al. Anti-BCMA CAR T-Cell Therapy bb2121 in Relapsed or Refractory Multiple Myeloma. *N Engl J Med*. 2019;380(18):1726-1737. doi:10.1056/NEJMoa1817226

15. J.M. Grigor E, Fergusson D, Kekre N, et al. Risks and Benefits of Chimeric Antigen Receptor T-Cell (CAR-T) Therapy in Cancer: A Systematic Review and Meta-Analysis. *Transfusion Medicine Reviews*. 2019;33(2):98-110. doi:https://doi.org/10.1016/j.tmrv.2019.01.005

16. Fraietta JA, Lacey SF, Orlando EJ, et al. Determinants of response and resistance to CD19 chimeric antigen receptor (CAR) T cell therapy of chronic lymphocytic leukemia. *Nature Medicine*. 2018;24(5):563-571. doi:10.1038/s41591-018-0010-1

17. van Bruggen JAC, Martens AWJ, Fraietta JA, et al. Chronic lymphocytic leukemia cells impair mitochondrial fitness in $CD8^+$ T cells and impede CAR T-cell efficacy. *Blood*. 2019;134(1):44-58. doi:10.1182/blood.2018885863

18. Ventola CL. Cancer immunotherapy, part 2: Efficacy, safety, and other clinical considerations. *P T*. 2017;42(7):452-463.

19. Guedan S, Ruella M, June CH. Emerging Cellular Therapies for Cancer. *Annual Review of Immunology*. 2019;37(1):145-171. doi:10.1146/annurev-immunol-042718-041407

20. Wagner J, Wickman E, DeRenzo C, Gottschalk S. CAR T Cell Therapy for Solid Tumors: Bright Future or Dark Reality? *Molecular Therapy*. 2020;28(11):2320-2339. doi:10.1016/j.ymthe.2020.09.015

21. Angajala A, Lim S, Phillips JB, et al. Diverse Roles of Mitochondria in Immune Responses: Novel Insights Into Immuno-Metabolism. *Frontiers in Immunology*. 2018;9. doi:10.3389/fimmu.2018.01605

22. Skanland SS, Brown JR. PI3K inhibitors in chronic lymphocytic leukemia: where do we go from here? *Haematologica*. Published online 2022. doi:10.3324/haematol.2022.281266

23. Lampson BL, Kasar SN, Matos TR, et al. Idelalisib given front-line for treatment of chronic lymphocytic leukemia causes frequent immune-mediated hepatotoxicity. *Blood*. 2016;128(2):195-203. doi:10.1182/blood-2016-03-707133

24. Patel K, Danilov AV, Pagel JM. Duvelisib for CLL/SLL and follicular non-Hodgkin lymphoma. *Blood*. 2019;134(19):1573-1577. doi:10.1182/blood.2019001795

25. Petersen CT, Hassan M, Morris AB, et al. Improving T-cell expansion and function for adoptive T-cell therapy using ex vivo treatment with PI3Kδ inhibitors and VIP antagonists. *Blood Advances*. 2018;2(3):210-223. doi:10.1182/bloodadvances.2017011254

26. Funk CR, Wang S, Chen KZ, et al. PI3Kδ/γ inhibition promotes human CART cell epigenetic and metabolic reprogramming to enhance antitumor cytotoxicity. *Blood*. 2022;139(4):523-537. doi:10.1182/blood.2021011597

27. Benard G, Bellance N, James D, et al. Mitochondrial bioenergetics and structural network organization. *Journal of Cell Science*. 2007;120(5):838-848. doi:10.1242/jcs.03381

28. Suen D-F, Norris KL, Youle RJ. Mitochondrial dynamics and apoptosis. *Genes & Development*. 2008;22(12):1577-1590. doi:10.1101/gad.1658508

29. Xie L, Shi F, Tan Z, Li Y, Bode AM, Cao Y. Mitochondrial network structure homeostasis and cell death. *Cancer Science*. 2018;109(12):3686-3694. doi:10.1111/cas.13830

30. Chandel NS. Evolution of Mitochondria as Signaling Organelles. *Cell Metabolism*. 2015;22(2):204-206. doi:10.1016/j.cmet.2015.05.013

31. Tan JX, Finkel T. Mitochondria as intracellular signaling platforms in health and disease. *Journal of Cell Biology*. 2020;219(5). doi:10.1083/jcb.202002179

32. Detmer SA, Chan DC. Functions and dysfunctions of mitochondrial dynamics. *Nature Reviews Molecular Cell Biology*. 2007;8(11):870-879. doi:10.1038/nrm2275

33. Chen H, Detmer SA, Ewald AJ, Griffin EE, Fraser SE, Chan DC. Mitofusins Mfn1 and Mfn2 coordinately regulate mitochondrial fusion and are essential for embryonic development . *Journal of Cell Biology*. 2003;160(2):189-200. doi:10.1083/jcb.200211046

34. S. Shirihai O, Song M, W. Dorn G. How Mitochondrial Dynamism Orchestrates Mitophagy. *Circulation Research*. 2015;116(11):1835-1849. doi:10.1161/CIRCRESAHA.116.306374

35. Perfettini J-L, Roumier T, Kroemer G. Mitochondrial fusion and fission in the control of apoptosis. *Trends in Cell Biology*. 2005;15(4):179-183. doi:10.1016/j.tcb.2005.02.005

36. Buck MD, O'Sullivan D, Klein Geltink RI, et al. Mitochondrial Dynamics Controls T Cell Fate through Metabolic Programming. *Cell*. 2016;166(1):63-76. doi:10.1016/j.cell.2016.05.035

37. Fannjiang Y, Cheng W-C, Lee SJ, et al. Mitochondrial fission proteins regulate programmed cell death in yeast. *Genes & Development*. 2004;18(22):2785-2797. doi:10.1101/gad.1247904

38. Yao C-H, Wang R, Wang Y, et al. Mitochondrial fusion supports increased oxidative phosphorylation during cell proliferation. *eLife*. 2019;8:e41351. doi:10.7554/eLife.41351

39. Cogliati S, Frezza C, Soriano ME, et al. Mitochondrial Cristae Shape Determines Respiratory Chain Supercomplexes Assembly and Respiratory Efficiency. *Cell*. 2013;155(1):160-171. doi:10.1016/j.cell.2013.08.032

40. Santel A, Frank S, Gaume B, Herrler M, Youle RJ, Fuller MT. Mitofusin-1 protein is a generally expressed mediator of mitochondrial fusion in mammalian cells. *Journal of Cell Science*. 2003;116(13):2763-2774. doi:10.1242/jcs.00479

41. Lanna A, Dustin ML. Mitochondrial fusion fuels T cell memory. *Cell Research*. 2016;26(9):969-970. doi:10.1038/cr.2016.94

42. Filadi R, Pendin D, Pizzo P. Mitofusin 2: from functions to disease. *Cell Death & Disease*. 2018;9(3):330. doi:10.1038/s41419-017-0023-6

43. Nunnari J, Suomalainen A. Mitochondria: In Sickness and in Health. *Cell*. 2012;148(6):1145-1159. doi:10.1016/j.cell.2012.02.035

44. Chan D, Frank S, Rojo M. Mitochondrial dynamics in cell life and death. *Cell Death & Differentiation*. 2006;13(4):680-684. doi:10.1038/sj.cdd.4401857

45. Chen H, Chomyn A, Chan DC. Disruption of Fusion Results in Mitochondrial Heterogeneity and Dysfunction. *Journal of Biological Chemistry*. 2005;280(28):26185-26192. doi:10.1074/jbc.M503062200

46. Vardhana SA, Hwee MA, Berisa M, et al. Impaired mitochondrial oxidative phosphorylation limits the self-renewal of T cells exposed to persistent antigen. *Nature Immunology*. 2020;21(9):1022-1033. doi:10.1038/s41590-020-0725-2

47. Eura Y, Ishihara N, Yokota S, Mihara K. Two Mitofusin Proteins, Mammalian Homologues of FZO, with Distinct Functions Are Both Required for Mitochondrial Fusion. *The Journal of Biochemistry*. 2003;134(3):333-344. doi:10.1093/jb/mvg150

48. Legros F, Lombès A, Frachon P, Rojo M. Mitochondrial Fusion in Human Cells Is Efficient, Requires the Inner Membrane Potential, and Is Mediated by Mitofusins. *MBoC*. 2002;13(12):4343-4354. doi:10.1091/mbc.e02-06-0330

49. Rojo M, Legros F, Chateau D, Lombès A. Membrane topology and mitochondrial targeting of mitofusins, ubiquitous mammalian homologs of the transmembrane GTPase Fzo. *Journal of Cell Science*. 2002;115(8):1663-1674. doi:10.1242/jcs.115.8.1663

50. Santel A, Fuller MT. Control of mitochondrial morphology by a human mitofusin. *Journal of Cell Science*. 2001;114(5):867-874. doi:10.1242/jcs.114.5.867

51. Koshiba T, Detmer SA, Kaiser JT, Chen H, McCaffery JM, Chan DC. Structural Basis of Mitochondrial Tethering by Mitofusin Complexes. *Science*. 2004;305(5685):858-862. doi:10.1126/science.1099793

52. Cao Y-L, Meng S, Chen Y, et al. MFN1 structures reveal nucleotide-triggered dimerization critical for mitochondrial fusion. *Nature*. 2017;542(7641):372-376. doi:10.1038/nature21077

53. Franco A, Kitsis RN, Fleischer JA, et al. Correcting mitochondrial fusion by manipulating mitofusin conformations. *Nature*. 2016;540(7631):74-79. doi:10.1038/nature20156

54. Qi Y, Yan L, Yu C, et al. Structures of human mitofusin 1 provide insight into mitochondrial tethering. *Journal of Cell Biology*. 2016;215(5):621-629. doi:10.1083/jcb.201609019

55. Hoppins S, Edlich F, Cleland MM, et al. The Soluble Form of Bax Regulates Mitochondrial Fusion via MFN2 Homotypic Complexes. *Molecular Cell*. 2011;41(2):150-160. doi:10.1016/j.molcel.2010.11.030

56. Daumke O, Roux A. Mitochondrial Homeostasis: How Do Dimers of Mitofusins Mediate Mitochondrial Fusion? *Current Biology*. 2017;27(9):R353-R356. doi:10.1016/j.cub.2017.03.024

57. Cipolat S, de Brito OM, Dal Zilio B, Scorrano L. OPA1 requires mitofusin 1 to promote mitochondrial fusion. *Proceedings of the National Academy of Sciences*. 2004;101(45):15927-15932. doi:10.1073/pnas.0407043101

58. Ge Y, Shi X, Boopathy S, et al. Two forms of Opa1 cooperate to complete fusion of the mitochondrial inner-membrane. *eLife*. 2020;9:e50973. doi:10.7554/eLife.50973

59. Richter V, Singh AP, Kvansakul M, Ryan MT, Osellame LD. Splitting up the powerhouse: structural insights into the mechanism of mitochondrial fission. *Cellular and Molecular Life Sciences*. 2015;72(19):3695-3707. doi:10.1007/s00018-015-1950-y

60. Ren L, Chen X, Chen X, Li J, Cheng B, Xia J. Mitochondrial Dynamics: Fission and Fusion in Fate Determination of Mesenchymal Stem Cells. *Frontiers in Cell and Developmental Biology*. 2020;8. doi:10.3389/fcell.2020.580070

61. Ren Z, Zhang X, Ding T, et al. Mitochondrial Dynamics Imbalance: A Strategy for Promoting Viral Infection. *Frontiers in Microbiology*. 2020;11. doi:10.3389/fmicb.2020.01992

62. Zacharioudakis E, Agianian B, Kumar MV V, et al. Modulating mitofusins to control mitochondrial function and signaling. *Nature Communications*. 2022;13(1):3775. doi:10.1038/s41467-022-31324-1

63. Anderson AC, Joller N, Kuchroo VK. Lag-3, Tim-3, and TIGIT: Co-inhibitory Receptors with Specialized Functions in Immune Regulation. *Immunity*. 2016;44(5):989-1004. doi:10.1016/j.immuni.2016.05.001

64. Baixauli F, Piletic K, Puleston DJ, et al. An LKB1–mitochondria axis controls TH17 effector function. *Nature*. 2022;610(7932):555-561. doi:10.1038/s41586-022-05264-1

65. Hong HS, Mbah NE, Shan M, et al. OXPHOS promotes apoptotic resistance and cellular persistence in TH17 cells in the periphery and tumor microenvironment. *Science Immunology*. 2022;7(77):eabm8182. doi:10.1126/sciimmunol.abm8182

66. Chen, K. Modulating Mitofusins to Enhance Therapeutic T Cell Expansion and Persistence. *Emory Theses and Dissertations*.